Research Article

MOLECULAR PAIN

Molecular Pain
Volume 13: 1–10

DOI: 10.1177/1744806916688016
journals.sagepub.com/home/mpx
SAGE

Dendritic spine dysgenesis in superficial dorsal horn sensory neurons after spinal cord injury

Xiaoyu C Cao[1,2], Laura W Pappalardo[1,2], Stephen G Waxman[1,2] and Andrew M Tan[1,2]

Abstract

Neuropathic pain is a major complication of spinal cord injury, and despite aggressive efforts, this type of pain is refractory to available clinical treatment. Our previous work has demonstrated a structure–function link between dendritic spine dysgenesis on nociceptive sensory neurons in the intermediate zone, laminae IV/V, and chronic pain in central nervous system and peripheral nervous system injury models of neuropathic pain. To extend these findings, we performed a follow-up structural analysis to assess whether dendritic spine remodeling occurs on superficial dorsal horn neurons located in lamina II after spinal cord injury. Lamina II neurons are responsible for relaying deep, delocalized, often thermally associated pain commonly experienced in spinal cord injury pathologies. We analyzed dendritic spine morphometry and localization in tissue obtained from adult rats exhibiting neuropathic pain one-month following spinal cord injury. Although the total density of dendritic spines on lamina II neurons did not change after spinal cord injury, we observed an inverse relationship between the densities of thin- and mushroom-shaped spines: thin-spine density decreased while mushroom-spine density increased. These structural changes were specifically noted along dendritic branches within 150 μm from the soma, suggesting a possible adverse contribution to nociceptive circuit function. Intrathecal treatment with NSC23766, a Rac1-GTPase inhibitor, significantly reduced spinal cord injury-induced changes in both thin- and mushroom-shaped dendritic spines. Overall, these observations demonstrate that dendritic spine remodeling occurs in lamina II, regulated in part by the Rac1-signaling pathway, and suggests that structural abnormalities in this spinal cord region may also contribute to abnormal nociception after spinal cord injury.

Keywords

spinal cord injury, dendritic spines, lamina II, superficial dorsal horn, pain, central sensitization

Date received: 8 September 2016; revised: 24 October 2016; accepted: 7 December 2016

Introduction

A common observation in neuropathic pain is the manifestation of central sensitization, which is characterized by excessive, abnormal electrical activity within sensory circuits.[1,2] Many factors contribute to nociceptive hyperexcitability including dysregulation of gene expression, loss of inhibitory control (e.g., interneuron cell death), and synaptic plasticity.[3–6] Less explored is the role of dendritic spine plasticity, specifically in chronic neurological diseases such as neuropathic pain. Dendritic spines are microscopic, specialized synaptic structures that serve as sites of excitatory input and are crucial elements in normal synaptic transduction.[7,8] Importantly, malformed dendritic spines in cortical tissue have been observed in a wide spectrum of neuropsychiatric and cognitive diseases, strongly suggesting that abnormal spine structure is directly related to abnormal function.[9]

A number of important studies have investigated changes in dendritic spine morphology in the brain after spinal cord injury (SCI).[10,11] However, few have

[1]Department of Neurology, Center for Neuroscience and Regeneration Research, Yale University School of Medicine, New Haven, CT, USA
[2]Rehabilitation Research Center, Veterans Affairs Connecticut Healthcare System, West Haven, CT, USA

Corresponding author:
Andrew M Tan, Department of Neurology, Center for Neuroscience and Regeneration Research, Yale University School of Medicine, 127A, 950 Campbell Avenue, Building 34, West Haven, CT 06516, USA.
Email: andrew.tan@yale.edu

investigated dendritic spine changes within the injured spinal cord. Our previous SCI studies have demonstrated that injury can lead to dendritic spine dysgenesis on wide-dynamic range (WDR) neurons within the deeper intermediate zone (laminae IV–VI) of the gray matter, and that this plasticity may directly contribute to the presence of neuropathic pain after SCI.[12–14] WDR neurons are of specific interest because they relay peripheral sensory information through the spinothalamic tract, a major pain pathway from the spinal cord to the brain. Disruption of dendritic spine remodeling after SCI with NSC23766, a potent inhibitor of Rac1-GTPase signaling involved in regulating the actin cytoskeleton, partially reduced both tactile allodynia and heat hyperalgesia.[12] While this previous study demonstrated that Rac1-regulated dendritic spine remodeling in laminae IV-VI can contribute to neuropathic pain after SCI, the role of dendritic spines in other regions of the nociceptive system were not explored. The superficial dorsal horn (lamina II) within the spinal cord is also a significant site of pain transmission and modulation. Lamina II neurons directly receive C- and Aδ-afferent terminal input from skin, muscle, and visceral organs, and thus are important for the initial processing of pain.[15–17] Notably, unmyelinated C-fibers comprise approximately 70% of nociceptive afferents and terminate primarily in lamina II.[18,19] Thus, lamina II neuronal circuits are responsible for processing delocalized and often thermally associated pain commonly experienced in SCI pathologies. An investigation of plasticity and remodeling of circuits in lamina II is therefore of high importance in elucidating mechanisms that contribute to chronic, pathological pain.

In this present study, we performed a retrograde analysis of dendritic spines in lamina II of spinal cord tissue collected from adult rats with SCI exhibiting neuropathic allodynia and hyperalgesia.[12] This study was made possible by leveraging the unique advantage of the Golgi-staining method, which preserves spinal cord tissues with archival grade durability with no degradation in the integrity of microscopic neuronal structures. Our observations show two structural abnormalities which may further reveal underlying factors that contribute to pathological excitability and nociception: first, lamina II neurons exhibit a ''switch'' from thin- to mushroom-shaped spines, and second, spine density increased preferentially on dendritic branch regions closest to the cell body. Within injured spinal cord tissue from animals that had received Rac1-GTPase inhibitor treatment, there was a significant attenuation of lamina II dendritic spine dysgenesis. This is the first report that profiles dendritic spine behavior in lamina II after injury and suggests that abnormal dendritic spine morphology in multiple regions[12] of the spinal dorsal horn may have a mechanistic relationship with abnormal pain.

Materials and methods

Animals

Experiments were performed in accordance with National Institutes of Health Guidelines for the Care and Use of Laboratory Animals and were approved by the Yale University Institutional Animal Use Committee (IACUC). Spinal cord tissue analyzed in this study was obtained from adult male Sprague Dawley rats (175–200 g), which had undergone SCI and drug treatments described in a previous study.[12]

Spinal cord injury

Briefly, rats were anesthetized with a mixture of ketamine and xylazine (80/5 mg/kg, i.p.) and subjected to a low thoracic (T9) spinal cord contusion injury using the New York University (NYU) impact injury device.[20] After laminectomy, a 2.0-mm diameter (10 g) rod was dropped from a 25-mm height onto the exposed section of spinal cord ($n = 32$). Intact Sham animals ($n = 14$) received laminectomy only. Post-operatively, all groups were administered twice daily subcutaneous injections of sterile saline solution (0.9%) and Baytril (0.3 cc; 22.7 mg/mL) for rehydration and prevention of bladder infection. Post-SCI recovery time lasted approximately 10 days, during which bladders were manually expressed twice a day until reflex function was restored.

Intrathecal Rac1 drug administration

Four weeks after SCI, a subpopulation of animals was anesthetized with a mixture of ketamine and xylazine (80/5 mg/kg, i.p.), and a sterile 32-gauge intrathecal catheter (ReCathCo, Allison Park, PA) was inserted through the atlanto-occipital membrane between the base of the skull and spinal vertebra C1.[12] The catheter was threaded caudally to the lumbar enlargement and secured with sutures. The rostral end of the catheter was heat-sealed to prevent cerebrospinal fluid leakage and infection. Under halothane sedation (<2 min, 3% by chamber), 5 μL (1 mg/mL) of Rac1 GTPase inhibitor, NSC23766 (EMD Chemicals, Darmstadt, Germany), was injected through the catheter followed by a 0.9% sterile saline flush (20 μL) ($n = 16$ animals, treatment group). The infusion was administered twice per day for three days. Control animals ($n = 16$) were administered a vehicle of 0.9% sterile saline.[12] This produced three comparator groups for this study: Sham, SCI + Vehicle, and SCI + NSC23766.

Golgi-staining and histology

Rats from the three treatment groups (Sham, SCI + Vehicle, and SCI + NSC23766) were sacrificed

one month after SCI or Sham surgeries. Fresh, unfixed spinal cord tissue from the lumbar enlargement (L3–L6) was removed, washed in distilled water, and placed into impregnation solutions. Golgi-cox staining was performed using the FD Rapid GolgiStain kit (FD Neurotechnologies, Columbia, MD) following the manufacturer's instructions. Coronal tissue sections (200 μm thick) were cut on a vibratome, mounted on gelatinized glass slides, rinsed in distilled water, dehydrated, cleared, and immobilized with Permount solution and a coverslip.[12] These mounted tissue samples were allowed to completely dry before any image analysis was performed.

In regards to this retrograde anatomical investigation, we confirmed the archival durability of our Golgi-staining approach using a light microscope to examine the integrity of these tissues approximately nine years later. As expected, we observed no degradation of the quality of fine microstructures on WDR neurons that were analyzed in the previous study.[12]

Neuron imaging and identification

Golgi-stained tissue sections were examined under standard light microscopy using a Nikon Eclipse E800 microscope with a HQ CoolSNAP camera (Roper Scientific, Tucson, AZ). Five morphological criteria were applied based on an adaptation of previous methodologies;[14,21] to identify putative excitatory superficial dorsal horn neurons for tracing: (1) neurons must be located within lamina II in the superficial dorsal horn (approximately 500 μm deep); (2) Golgi-stained neurons must have dendrites that are completely impregnated and appeared as a continuous length; (3) neurons must have at least three primary dendrites extending from the cell body, although branching was not required; (4) dendritic trees must extend in all directions, i.e., "radially" (a specific morphological distinction between excitatory and inhibitory neurons in the superficial dorsal horn; see Yasaka et al.[21]); and (5) the cell body diameter must fall between 20 and 50 μm. Note that while the neurons classified by Yasaka et al.[21] were viewed in the sagittal plane, we expected that the use of coronal sections in this study would not confound the identification of excitatory neurons, as dendritic trees would extend radially in all three dimensions. A total of 75 excitatory lamina II neurons ($n = 25$ per group) were identified using these criteria and included in this analysis. The data for other morphological characteristics of sampled neurons are located in Table 1.

Dendritic spine identification and morphological classification

Dendritic spines were identified and classified using profile information from Kim et al.[11] Briefly, a protrusion from the dendrite branch was considered a spine only if a clear neck structure was present. If no clear neck structure was observed, then the protrusion was considered a spine when we observed concave indentations on both sides of the juxtaposed protrusion and the dendritic branch. Classification of dendritic spines into "thin" and "mushroom" morphologies was performed as follows: spines with head-like enlargements with diameter less than the length of the neck were considered thin spines, whereas spines with head diameters exceeding the neck length were considered mushroom spines.[14] Neck length was defined as the length from the spine-dendrite branch junction to the base of the spine head. This classification approach was validated based on three reasons: (1) the use of only two distinct morphological classifications provides for simple yet strict guidelines for classifying spines; (2) the large number of spines included in this study ($n = 25{,}348$) precluded the need to distinguish between slight variations in spine shape; and (3) a substantial body of literature has catalogued the different physiological characteristics of dendritic spines with thin- and mushroom-shaped morphologies.[22]

Dendritic spine analysis

All analyses of dorsal horn neurons were accomplished by a blinded observer using Neurolucida

Table 1. Comparison of cell body dimensions and dendritic tree morphology.

	Maximum diameter of cell body (μm)	Total dendrite length (μm)	Number of primary dendrites	Length of primary dendrite (μm)	Primary dendrites with secondary branches (%)	Depth of neuron dorsal spinal cord surface (μm)
Sham	24.4 ± 2.2	1016.4 ± 133.3	5.0 ± 0.5	69.8 ± 10.5	59.4 ± 7.3	550 ± 21
SCI + vehicle	27.2 ± 1.7	1349.7 ± 140.5	4.7 ± 0.4	68.1 ± 9.9	58.6 ± 6.1	536 ± 18
SCI + NSC23766	27.0 ± 1.3	1118.7 ± 122.3	4.5 ± 0.3	87.2 ± 10.3	50.5 ± 6.3	542 ± 13

SCI: spinal cord injury.

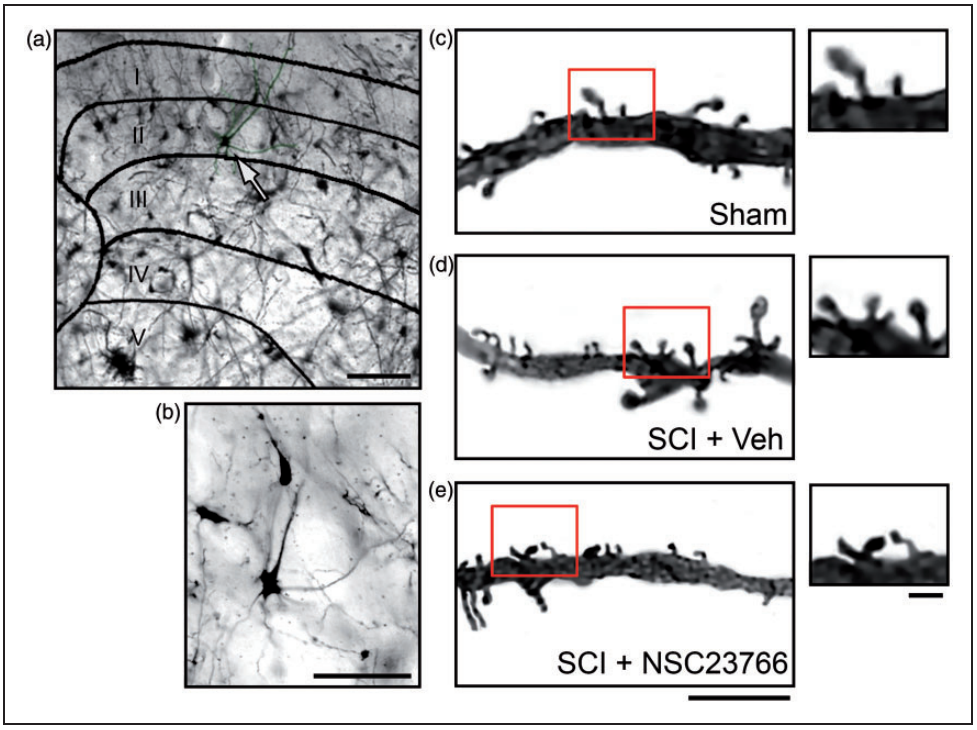

Figure 1. Golgi-stained tissue from lumbar spinal cord. (a) Cross section of spinal cord with a representative neuron from a Sham animal (white arrow). (b) Magnified view of representative neuron from (a) (white arrow). Representative samples of dendritic branches and spines from Sham (c), SCI + Vehicle (d), and SCI + NSC23766 (e). (c)–(e) Magnified view of spines on dendritic branches (see red box). Scale bars in (a) = 100 μm; (b) = 50 μm; (c)–(e) = 10 μm and 1 μm.

software (MicroBrightField Biosciences, Williston, VT). First, the contours of coronal spinal cord sections and spinal cord gray matter were digitally traced and locations of sampled neurons in the lamina II region were marked. A three-dimensional reconstruction of each candidate neuron was then rendered through the *x*-, *y*-, and *z*-axes. Dendritic spines with thin- and mushroom-shaped profiles were marked along these reconstructions. Using NeuroExplorer software, the spine density and spine distribution relative to the soma were calculated. Datasets were subsequently compared across treatment groups.

Statistical analysis

Statistical significance was determined using parametric or non-parametric statistical tests at the α-level of significance of $p = 0.05$. Statistical tests included one-way analysis of variance (ANOVA) or ANOVA on ranks followed by post hoc tests to control for repeated measure errors, e.g., Bonferonni's or Dunn's test, as appropriate. Data management was performed using Microsoft Office Excel 2011 (Microsoft, Redmond, WA), and statistical analyses were performed using SigmaPlot (version 13.0; Systat Software Inc.) Numerical data in the text and graphs are presented as mean ± standard error of the mean (SEM). Data in Table 1 are presented as mean ± standard deviation (SD).

Results

Dendritic spines reorganize on lamina II neurons after SCI

Excitatory lamina II neurons were identified (with morphological profiles shown in Table 1) from Golgi-stained spinal cord tissue and reconstructed with Neurolucida software (Figures 1 and 2; $n = 25$ cells/group). These tissues were collected from animals one month after SCI or Sham surgeries. For morphological analysis, the spinal cord and gray matter contours were first traced to record the anatomical region of sampled lamina II neurons (contours not shown; Figures 1(a)–(c) and 2(a)–(c)). Neurons were sampled in three dimensions, with thin- and mushroom-shaped spines marked with blue and red dots, respectively (Figure 2(a)–(c), lower panels). In our previous study of WDR neurons located in deep lamina (IV–VI), total thin- and mushroom-shaped dendritic spine densities increased following SCI.[12] Thus, we expected to observe similar results in lamina II neurons.

However, in contrast to these previous findings, there was no significant difference in total spine density

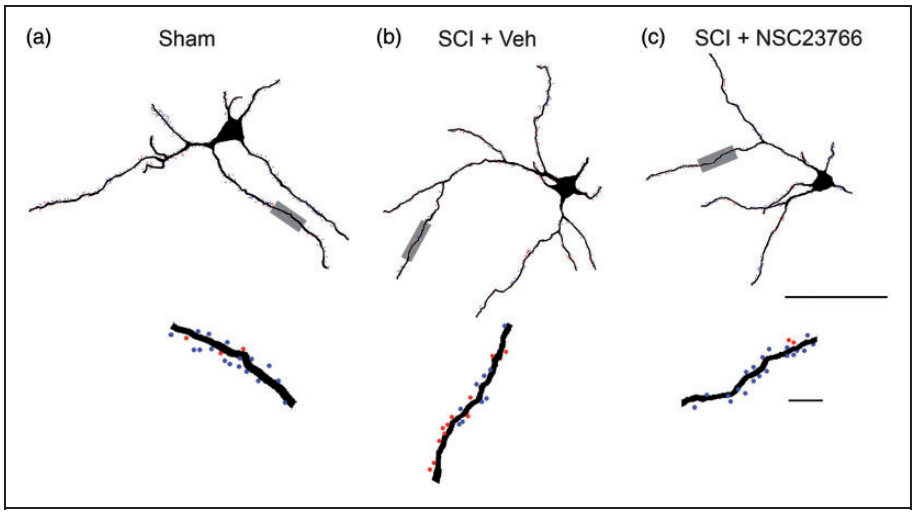

Figure 2. Digital reconstructions of lamina II neurons. Renderings show the morphology of representative neurons from each treatment group: Sham (a), SCI + Vehicle (b), and SCI + NSC23766 (c) (bottom panels in (a)–(c)). Magnified view of a dendritic branch segment with thin (blue dots) and mushroom (red dots) spines. Scale bars in ((a)–(c)) =50 μm and 10 μm.

between the three treatment groups (Figure 3(a)). As shown in Figure 3(a), total spine density for each treatment group was expressed as the number of all spines per 10 μm dendritic length, pooled within groups, and statistically compared across treatment groups ($p > 0.05$; one-way ANOVA with Bonferroni's post hoc; Sham: 3.3 ± 0.16; SCI + Veh: 2.6 ± 0.21; SCI + NSC23766: 3.37 ± 0.32 spines/10 μm dendrite). Interestingly, we did observe an inverse quantitative change between the densities of thin- and mushroom-shaped dendritic spines after SCI (Figure 2(b) and (c)). Whereas thin-shaped spine density significantly decreased as compared with Sham, mushroom-shaped spines increased after SCI ($p < 0.01$; SCI + Veh vs. Sham: 1.35 ± 0.10 vs. 2.51 ± 0.13 thin spines/10 μm dendrite; SCI + Veh vs. Sham: 1.26 ± 0.13 vs. 0.56 ± 0.07 mushroom spines/10 μm dendrite).

In animals treated with the Rac1-inhibitor, NSC23766, after SCI, we observed no effect on total spine density when this group was compared with Sham- or vehicle-treated SCI animals ($p > 0.05$). NSC23766 treatment significantly increased thin-shaped spine density compared with SCI + Vehicle (Figure 3(b)) ($p < 0.01$; 2.59 ± 0.26 vs.1.35 ± 0.10 thin spines/10 μm dendrite, respectively), but was not different from uninjured Sham levels ($p > 0.05$). NSC23766 also reduced mushroom-shaped spine density compared to SCI + Vehicle animals (Figure 3(c)) ($p < 0.01$; 0.79 ± 0.08 vs. 1.26 ± 0.13 mushroom spines/10 μm dendrite. As with thin-shaped spines, we also did not find a difference between mushroom-shaped spine densities in NSC23766-treated SCI animals and Sham ($p > 0.05$). Together, this dataset suggests an inverse relationship between morphological subtypes of dendritic spines in lamina II neurons after SCI: thin-shaped spine density decreased, while mushroom-shaped spine density increased.

Spines redistribute along the dendritic branch relative to the soma after SCI

The location of spines on the dendritic branch has functional implications on neuronal output and circuit physiology.[23] A significant body of work has shown that excitatory afferent input to dendritic branches closer to the cell body have more impact upon excitatory postsynaptic potential (EPSP) generation than those inputs located farther away.[24–27] In the intermediate zone of the dorsal horn (lamina IV and VI), dendritic spines on WDR neurons undergo spatial redistribution following SCI and peripheral nerve injury,[12,28] and these changes are associated with central sensitization and neuropathic pain. To follow-up on these studies, we assessed whether a similar dendritic spine redistribution occurred on superficial neurons in lamina II. We examined SCI-induced redistribution of spines along dendritic branches of lamina II neurons using a Sholl's analysis to compare spine densities across treatment groups at corresponding 50 -μm-wide regions relative to the soma, up to 400 μm away from the cell body (Figure 4). Total spine density did not change significantly after SCI at any region for any group, as compared with Sham (Figure 4(a)) ($p > 0.05$; Sham vs. SCI + vehicle, or SCI + vehicle vs. SCI + NSC23766 at any region 50–400 μm). In contrast, thin-shaped spine densities decreased in all regions within 150 μm of the soma after SCI, as compared to

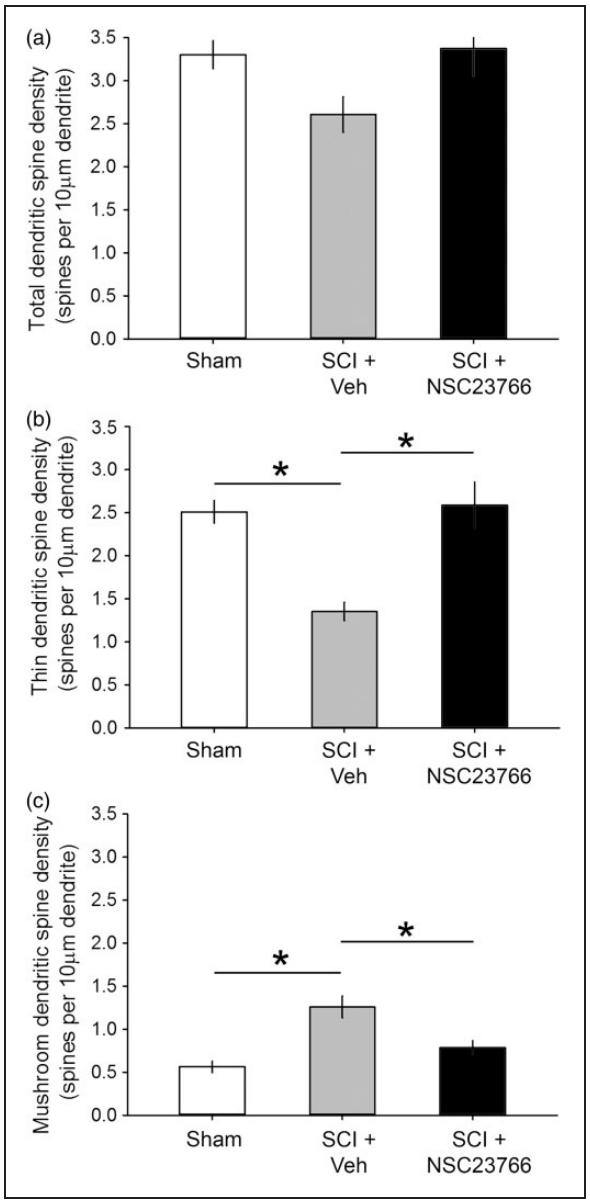

Figure 3. Dendritic spine density. (a) Total dendritic spine density was unchanged among the three experimental groups (n.s.; $p > 0.05$). (b) One month after SCI, thin spine density decreased as compared with Sham ($*p < 0.05$). (c) In contrast following SCI, mushroom spine density increased as compared with Sham ($*p < 0.05$). ((b), (c)) Treatment with NSC23766 restored both thin and mushroom spine densities close-to-Sham levels ($p > 0.05$). As shown in (a), there was no effect of NSC23766 treatment on total spine density. Data are shown as mean ± SEM.

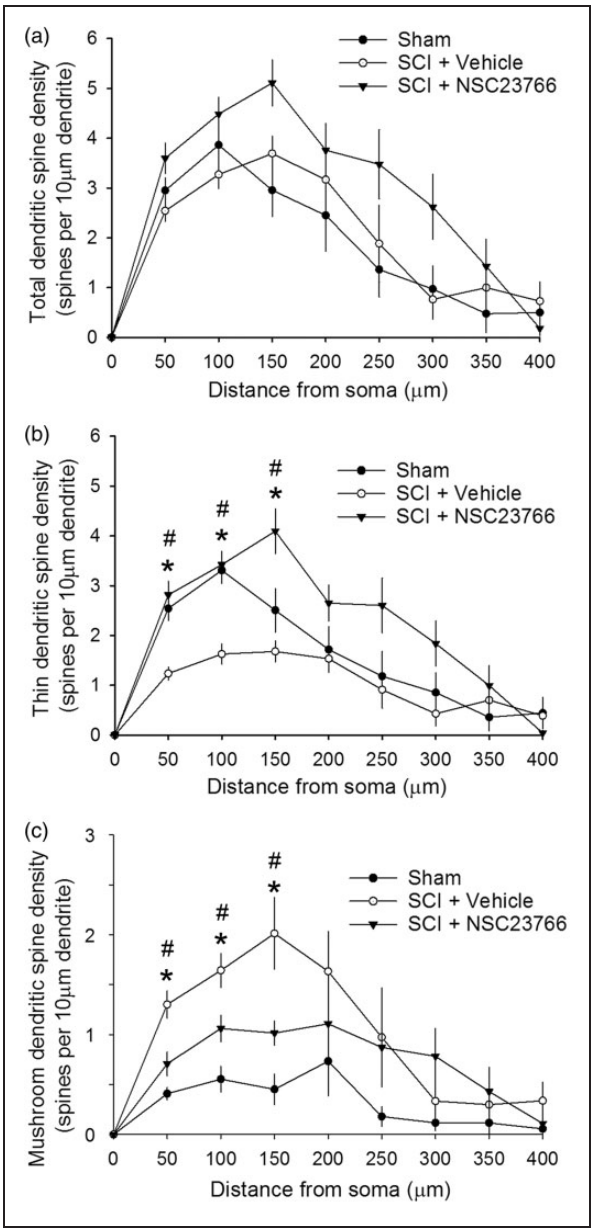

Figure 4. Spatial distribution of dendritic spines. (a) Thin and (b) mushroom spine densities increase significantly at regions closest to the soma after SCI as compared with Sham ($*p < 0.05$). ((b), (c)) Treatment with NSC23766 partially reduced these changes in thin and mushroom spines close-to-Sham levels. Moreover, NSC23766 treatment in SCI animals increased thin-shaped spines and decreased mushroom-shaped spines as compared with SCI animals and vehicle treatment only ($\#p < 0.05$). As shown in (a), total spine densities do not change significantly at any dendritic region after SCI. Data are shown as mean ± SEM.

Sham (Figure 4(b)) ($p < 0.05$, ANOVA on ranks with Dunn's post hoc test; at 50 μm: 1.23 ± 0.13 vs. 2.54 ± 0.24; at 100 μm: 1.6 ± 0.20 vs. 3.31 ± 0.27; at 150 μm: 1.68 ± 0.21 vs. 2.5 ± 0.43 thin spines/10 μm dendrite). Mushroom spine densities increased significantly in similar regions as compared with Sham (Figure 4(c)) ($p < 0.05$, ANOVA on ranks with Dunn's post hoc test; at 50 μm: 1.3 ± 0.14 vs. 0.41 ± 0.06; at 100 μm: 0.55 ± 0.13 vs. 1.64 ± 0.17; at 150 μm: 0.45 ± 0.16 vs. 2.01 ± 0.36 mushroom spines/10 μm dendrite).

Treatment with the Rac1-inhibitor NSC23766 in SCI animals attenuated the overall injury-induced spatial redistribution of thin and mushroom spine densities observed after SCI (Figure 4(b) and (c)). Compared to SCI, NSC23766 treatment resulted in thin-spine densities that appeared close-to-Sham levels in proximal regions to the soma, within 150 μm of the soma (Figure 4(b)) ($p > 0.05$). Treatment with NSC23766 in SCI animals significantly increased thin-shaped spines as compared with SCI + Vehicle at the regions between 50 and 150 μm from the soma ($p < 0.05$; ANOVA on ranks with Dunn's post hoc test; at 50 μm: 2.8 ± 0.27 vs. 1.24 ± 0.13; at 100 μm: 3.42 ± 0.27 vs. 1.62 ± 0.20; at 150 μm: 4.1 ± 0.45 vs. 1.68 ± 0.21 thin spines/10 μm dendrite). For mushroom-shaped spines, Rac1 inhibition resulted in a significant decrease in mushroom spine densities at the three regions closest to the soma as compared to SCI + Vehicle (Figure 4(c)) ($p < 0.05$; ANOVA on ranks with Dunn's post hoc test; at 50 μm: 0.71 ± 0.12 vs. 1.3 ± 0.14; at 100 μm: 1.06 ± 0.13 vs. 1.64 ± 0.17; at 150 μm: 1.01 ± 0.12 vs. 2.01 ± 0.36 mushroom spines/10 μm dendrite). NSC23766 treatment, however, did not fully restore mushroom-shaped spine densities back to Sham levels, as the SCI-induced increase in mushroom densities remained significantly different than sham ($p < 0.05$; SCI + NSC23766 vs. Sham; ANOVA on ranks with Dunn's post hoc test; at 50 μm: 0.71 ± 0.12 vs. 0.4 ± 0.06; at 100 μm: 1.06 ± 0.13 vs. 0.55 ± 0.13; at 150 μm: 1.01 ± 0.12 vs. 0.45 ± 0.15 mushroom spines/10 μm dendrite). At distances greater than 200 μm from the soma, there was no effect of SCI or any treatment on the regional densities of thin, mushroom, or total spines—all SCI-induced changes occurred in regions close to the cell body.

Discussion

The majority of excitatory synapses within the central nervous system occur on dendritic spines.[22,29,30] In the current study, we performed an in-depth anatomical study of dendritic spines on lamina II neurons in post-mortem tissue obtained from animals with SCI and published electrophysiological and behavioral evidence of neuropathic allodynia and hyperalgesia.[12] This previous study demonstrated that Rac1-regulated dendritic spine remodeling on WDR neurons (located in deeper laminae IV-VI) has a potential mechanistic contribution to the development and maintenance of neuropathic pain.[12] An unanswered question posed by this prior work was whether lamina II neurons in animals with SCI-induced neuropathic pain also underwent dendritic spine plasticity. To address this unresolved issue, we retrogradely analyzed this archived Golgi-stained tissue.

We chose to perform this analysis of lamina II neurons for four primary reasons: first, the superficial dorsal horn is a major site of pain processing and transmission. Neurons of lamina II directly receive C- and Aδ-afferent terminal input from the periphery;[17,31] second, C-fibers comprise up to 70% of nociceptive afferents that synapse within lamina II;[18,19] third, it is well-established that lamina II neuronal circuits have a primary role in the processing of delocalized, thermal pain commonly experienced in SCI;[32–36] and finally, although the presence of dendritic spines in lamina II neurons has been documented,[21] there have been no studies of dendritic spine behavior in this region of the spinal cord, particularly following SCI. Because of the important role of lamina II circuitry in nociception, an understanding of injury-induced plasticity of dendritic spines would further contribute to elucidating mechanisms underlying neuropathic pain.

Previous work from our group has revealed a common motif of dendritic spine morphologies associated with neuronal hyperexcitability and pain.[9,14] Pain-associated dendritic spine profiles include an increase in spine density—especially mushroom-shaped spines—which represent more efficacious and stable synaptic connections as compared to thin- or "filopodia"-like spine structures, with a preferential redistribution of dendritic spines toward the neuron cell body. These pain-associated spine profiles appear to be conserved across several injury and disease models of neuropathic pain, including peripheral nerve injury, diabetes mellitus, severe cutaneous burn injury, and SCI.[37,38] Importantly, in all of these pain models, it was demonstrated that disruption of Rac1 is necessary and sufficient for both the reduction in dendritic spine dysgenesis and neuropathic pain. Rac1 activity has a significant role in regulating the actin filament cytoskeleton in dendritic spines and concomitantly promotes the clustering of AMPA receptors in the post-synaptic spine membrane.[39–41]

Here, we examined whether SCI-induced dendritic spine dysgenesis occurs in lamina II neurons of the superficial dorsal horn, and whether any changes are also mediated by Rac1-GTPase. In spinal cord tissue obtained one month after SCI, there were no significant changes detected in overall total spine density after SCI with or without NSC23766 (Rac1-inhibitor) treatment. However, when dendritic spines were categorized into thin and mushroom spines, we observed a morphological "switch." More specifically, in animals that had prior evidence of neuropathic pain after SCI,[12] there was an inverse relationship of dendritic spine morphologies in lamina II neurons: as thin-shaped spine density decreased, mushroom-shaped spine density increased. Although we are careful to avoid over-speculation, the shift in spine morphology from thin- to mushroom-shaped after SCI is consistent with the functional phenomenon of mushroom spines increasing neuronal

excitability.[23,42,43] The relatively larger volume of the mushroom spine head, upon which presynaptic elements terminate, strongly correlates with a larger post-synaptic density (PSD), an electron-dense matrix containing membrane proteins anchored to cytoskeletal molecules and glutamate receptors.[29] In computer-simulated environments, an increase in the spine head volume has been shown to increase EPSP amplitude, decrease time to peak (i.e., action potential wave "sharpness"), amplify background noise, and shorten the refractory period, which permits action potentials to fire at higher frequency.[23] Thus, in the case of superficial dorsal horn neurons, we interpret the increase in the prevalence of mushroom spines to be indicative of an increase in excitatory synaptic efficacy in lamina II nociceptive circuits.

In addition to calculating dendritic spine density, we also profiled changes in spine distribution along dendritic branches. The location of dendritic spines relative to the cell body has a significant physiological impact upon neurotransmission:[44–46] the distance of the dendritic spine from the soma is inversely related to the magnitude of any excitatory potential. In particular, computer simulations have demonstrated that EPSP peak amplitudes increase at a greater rate for each spatial unit closer to the cell body for mushroom spines than compared with thin spines.[23] In lamina II, dendritic spines preferentially increased in density along branch locations closest to the cell body after SCI. In contrast to our previous findings of deep lamina WDR neurons,[12] this preferential injury-induced distribution was only apparent in lamina II when thin and mushroom spines were analyzed as distinct subtypes. One month after SCI, thin-shaped spine density decreased in proximal regions, concomitant with an increase in mushroom-shaped spine density within the same region. Although overall spine number and position relative to the soma remained constant with SCI and Rac1-inhibition, our observations demonstrate the existence of a "spatial-dependent" attribute of dendritic spine remodeling in lamina II.

Pharmacological inhibition of Rac1, a small (~21 kDa) protein in the Rho family of GTPases, can partially reduce injury-associated changes to dendritic spine morphology and attenuate pain.[12,14,28] Moreover, viral-mediated over-expression of Rac1 in mice with a Kalirin-7 knockout in dorsal horn neurons enhanced CFA-induced mechanical hypersensitivity and increased dendritic spine density in the superficial spinal cord.[47] Thus, Rac1 along with Kalirin-7 may act together within the superficial dorsal horn to influence the manifestation of pain and dendritic spine reorganization. In our retro-analysis of Golgi-stained tissue, we expected that administration of NSC23766 would block abnormal, injury-induced dendritic spine remodeling in superficial lamina II, consistent with the effects of Rac1 inhibition in deeper laminae of the lumbar enlargement following SCI.[12] However, we did not observe whole cell effects of the drug on overall total, thin-, or mushroom-shaped spine densities. On the other hand, Rac1 inhibition did affect changes in the spatial distribution of spines along proximal regions of dendritic branches. Thin spine densities were completely restored to control levels, while mushroom spine densities were partially restored by NSC23766 treatment in regions less than 150 μm from the cell body. These results demonstrate that Rac1 signaling has a mechanistic contribution in structural reorganization of dendritic spines in lamina II after SCI. These observations together with previous studies suggest that Rac1 may contribute to dendritic spine remodeling following SCI in a contextual manner based on neuronal topography within the dorsal horn nociceptive system.

There are notable caveats to this study. Because a retro-analysis on Golgi-stained post-mortem tissue obtained from animals in a prior study was performed, we can only speculate as to the functional implications of the anatomical findings in lamina II within the context of the prior study.[12] We did not perform functional studies for this report. Additionally, given that administration of intrathecal NSC23766 is non-specific, we cannot preclude the possibility that pharmacological inhibition of Rac1 has non-neuronal effects (e.g. glia), which may be implicated in dendritic spine remodeling and/or neuropathic pain. A future approach to overcome current limitations of the present and previous studies is direct intracellular recording from single lamina II nociceptive neurons, combined with assessment of dendritic spine remodeling behavior. Additionally, *in vivo* multiphoton imaging[48,49] could help clarify the mechanistic relationship between dendritic spine plasticity in the superficial dorsal horn and neuropathic pain.

In summary, we report for the first time that dendritic spine remodeling occurs in dorsal horn lamina II, a region associated with nociception, following SCI. We also show that dendritic spines exhibit a morphological profile consistent with those observed in animals with neuropathic pain. Rac1 appears to have an important role in mediating these dendritic spine changes in the superficial dorsal horn. However, Rac1 signaling may have differential effects on dorsal horn dendritic spine morphogenesis in a contextual-based manner. Together, these results extend previous findings demonstrating that Rac1-mediated dendritic spine remodeling of neurons in the dorsal horn may contribute to neuropathic pain following SCI.

Author Contributions

XCC and LWP equally contributed to this work.

Declaration of Conflicting Interests

The author(s) declared no potential conflicts of interest with respect to the research, authorship, and/or publication of this article.

Funding

The author(s) disclosed receipt of the following financial support for the research, authorship, and/or publication of this article: This work was supported in part by grants from the Medical Research Service and Rehabilitation Research Service, Department of Veterans Affairs. The Center for Neuroscience and Regeneration Research is a Collaboration of the Paralyzed Veterans of America and the United Spinal Association with Yale University. AMT is funded through the generous support of the PVA Research Foundation, Taylor Foundation for Chronic Diseases, and a VA Career Development Award (1-IK2-RX-001123-01-A2). LWP is funded in part by the Yale MSTP training Grant (NGM007205). The authors thank Shujun Liu, Peng Zhao, and Myriam Hill for their excellent technical assistance.

References

1. Ali Z, Meyer RA and Campbell JN. Secondary hyperalgesia to mechanical but not heat stimuli following a capsaicin injection in hairy skin. *Pain* 1996; 68: 401–411.
2. Koltzenburg M, Torebjork HE and Wahren LK. Nociceptor modulated central sensitization causes mechanical hyperalgesia in acute chemogenic and chronic neuropathic pain. *Brain* 1994; 117(Pt 3): 579–591.
3. Cordero-Erausquin M, Coull JA, Boudreau D, et al. Differential maturation of GABA action and anion reversal potential in spinal lamina I neurons: impact of chloride extrusion capacity. *J Neurosci* 2005; 25: 9613–9623.
4. Kuner R. Central mechanisms of pathological pain. *Nat Med* 2010; 16: 1258–1266.
5. Mannion RJ, Costigan M, Decosterd I, et al. Neurotrophins: peripherally and centrally acting modulators of tactile stimulus-induced inflammatory pain hypersensitivity. *Proc Natl Acad Sci U S A* 1999; 96: 9385–9390.
6. Neumann S, Doubell TP, Leslie T, et al. Inflammatory pain hypersensitivity mediated by phenotypic switch in myelinated primary sensory neurons. *Nature* 1996; 384: 360–364.
7. Chen LY, Rex CS, Casale MS, et al. Changes in synaptic morphology accompany actin signaling during LTP. *J Neurosci* 2007; 27: 5363–5372.
8. Yuste R and Bonhoeffer T. Morphological changes in dendritic spines associated with long-term synaptic plasticity. *Ann Rev Neurosci* 2001; 24: 1071–1089.
9. Tan AM. Dendritic spine dysgenesis: An emerging concept in neuropsychiatric disease. *Neurosci Lett* 2015; 601: 1–3.
10. Kim BG, Dai HN, McAtee M, et al. Modulation of dendritic spine remodeling in the motor cortex following spinal cord injury: effects of environmental enrichment and combinatorial treatment with transplants and neurotrophin-3. *J. Comp. Neurol* 2008; 508: 473–486.
11. Kim BG, Dai HN, McAtee M, et al. Remodeling of synaptic structures in the motor cortex following spinal cord injury. *Exp Neurol* 2006; 198: 401–415.
12. Tan AM, Stamboulian S, Chang YW, et al. Neuropathic pain memory is maintained by Rac1-regulated dendritic spine remodeling after spinal cord injury. *J Neurosci* 2008; 28: 13173–13183.
13. Tan AM and Waxman SG. Spinal cord injury, dendritic spine remodeling, and spinal memory mechanisms. *Exp Neurol* 2012; 235: 142–151.
14. Zhao P, Hill M, Liu S, et al. Dendritic spine remodeling following early and late Rac1 inhibition after spinal cord injury: evidence for a pain biomarker. *J Neurophysiol* 2016; 115: 2893–2910.
15. Cervero F, Bennett GJ, Headley PM, et al. *Processing of sensory information in the superficial dorsal horn of the spinal cord*. Boston, MA: Springer US, 1989.
16. Todd AJ, Puskar Z, Spike RC, et al. Projection neurons in lamina I of rat spinal cord with the neurokinin 1 receptor are selectively innervated by substance p-containing afferents and respond to noxious stimulation. *J Neurosci* 2002; 22: 4103–4113.
17. Woolf CJ and Fitzgerald M. Somatotopic organization of cutaneous afferent terminals and dorsal horn neuronal receptive fields in the superficial and deep laminae of the rat lumbar spinal cord. *J Comp Neurol* 1986; 251: 517–531.
18. Nagy JI and Hunt SP. The termination of primary afferents within the rat dorsal horn: evidence for rearrangement following capsaicin treatment. *J Comp Neurol* 1983; 218: 145–158.
19. Todd AJ. Neuronal circuitry for pain processing in the dorsal horn. *Nature Rev Neurosci* 2010; 11: 823–836.
20. Hains BC and Waxman SG. Activated microglia contribute to the maintenance of chronic pain after spinal cord injury. *J Neurosci* 2006; 26: 4308–4317.
21. Yasaka T, Tiong SY, Hughes DI, et al. Populations of inhibitory and excitatory interneurons in lamina II of the adult rat spinal dorsal horn revealed by a combined electrophysiological and anatomical approach. *Pain* 2010; 151: 475–488.
22. Calabrese B, Wilson MS and Halpain S. Development and regulation of dendritic spine synapses. *Physiology (Bethesda)* 2006; 21: 38–47.
23. Tan AM, Choi JS, Waxman SG, et al. Dendritic spine remodeling after spinal cord injury alters neuronal signal processing. *J Neurophysiol* 2009; 102: 2396–2409.
24. Holthoff K and Tsay D. Calcium dynamics in spines: link to synaptic plasticity. *Exp Physiol* 2002; 87: 725–731.
25. Holthoff K, Tsay D and Yuste R. Calcium dynamics of spines depend on their dendritic location. *Neuron* 2002; 33: 425–437.
26. Rall W, Burke RE, Smith TG, et al. Dendritic location of synapses and possible mechanisms for the monosynaptic EPSP in motoneurons. *J Neurophysiol* 1967; 30: 1169–1193.
27. Yuste R and Urban R. Dendritic spines and linear networks. *J Physiol Paris* 2004; 98: 479–486.

28. Tan AM, Chang YW, Zhao P, et al. Rac1-regulated dendritic spine remodeling contributes to neuropathic pain after peripheral nerve injury. *Exp Neurol* 2011; 232: 222–233.
29. McKinney RA. Excitatory amino acid involvement in dendritic spine formation, maintenance and remodelling. *J Physiol* 2010; 588: 107–116.
30. Niesmann K, Breuer D, Brockhaus J, et al. Dendritic spine formation and synaptic function require neurobeachin. *Nat Commun* 2011; 2: 557.
31. Todd AJ. Anatomy of primary afferents and projection neurones in the rat spinal dorsal horn with particular emphasis on substance P and the neurokinin 1 receptor. *Exp Physiol* 2002; 87: 245–249.
32. Chen SR, Chen H, Yuan WX, et al. Increased presynaptic and postsynaptic {alpha}2-adrenoceptor activity in the spinal dorsal horn in painful diabetic neuropathy. *J Pharm Exp Ther* 2011; 337: 285–292.
33. Ikeda H, Stark J, Fischer H, et al. Synaptic amplifier of inflammatory pain in the spinal dorsal horn. *Science* 2006; 312: 1659–1662.
34. Sandkuhler J and Liu X. Induction of long-term potentiation at spinal synapses by noxious stimulation or nerve injury. *Eur J Neurosci* 1998; 10: 2476–2480.
35. Yasaka T, Tiong SY, Polgar E, et al. A putative relay circuit providing low-threshold mechanoreceptive input to lamina I projection neurons via vertical cells in lamina II of the rat dorsal horn. *Mol Pain* 2014; 10: 3.
36. Zhang L, Berta T, Xu ZZ, et al. TNF-alpha contributes to spinal cord synaptic plasticity and inflammatory pain: distinct role of TNF receptor subtypes 1 and 2. *Pain* 2011; 152: 419–427.
37. Tan AM. Dendritic spine dysgenesis in neuropathic pain. *Prog Mol Biol Transl Sci* 2015; 131: 385–408.
38. Tan AM and Waxman SG. Dendritic spine dysgenesis in neuropathic pain. *Neurosci Lett* 2015; 601: 54–60.
39. Duman JG, Tzeng CP, Tu YK, et al. The adhesion-GPCR BAI1 regulates synaptogenesis by controlling the recruitment of the Par3/Tiam1 polarity complex to synaptic sites. *J Neurosci* 2013; 33: 6964–6978.
40. Nishida H and Okabe S. Direct astrocytic contacts regulate local maturation of dendritic spines. *J Neurosci* 2007; 27: 331–340.
41. Wiens KM, Lin H and Liao D. Rac1 induces the clustering of AMPA receptors during spinogenesis. *J Neurosci* 2005; 25: 10627–10636.
42. Bourne J and Harris KM. Do thin spines learn to be mushroom spines that remember? *Curr Opin Neurobiol* 2007; 17: 381–386.
43. Harris KM, Jensen FE and Tsao B. Three-dimensional structure of dendritic spines and synapses in rat hippocampus (CA1) at postnatal day 15 and adult ages: implications for the maturation of synaptic physiology and long-term potentiation. *J Neurosci* 1992; 12: 2685–2705.
44. Pongracz F. The function of dendritic spines: a theoretical study. *Neuroscience* 1985; 15: 933–946.
45. Rusakov DA, Stewart MG and Korogod SM. Branching of active dendritic spines as a mechanism for controlling synaptic efficacy. *Neuroscience* 1996; 75: 315–323.
46. Segev I and Rall W. Computational study of an excitable dendritic spine. *J Neurophysiol* 1988; 60: 499–523.
47. Lu J, Luo C, Bali KK, et al. A role for Kalirin-7 in nociceptive sensitization via activity-dependent modulation of spinal synapses. *Nat Commun* 2015; 6: 6820.
48. Fenrich KK, Weber P, Hocine M, et al. Long-term in vivo imaging of normal and pathological mouse spinal cord with subcellular resolution using implanted glass windows. *J Physiol* 2012; 590: 3665–3675.
49. Fenrich KK, Weber P, Rougon G, et al. Long- and short-term intravital imaging reveals differential spatiotemporal recruitment and function of myelomonocytic cells after spinal cord injury. *J Physiol* 2013; 591: 4895–4902.